K-Ras and B-Raf oncogenes inhibit colon epithelial polarity establishment through up-regulation of c-myc

Kirti Magudia, Aurelia Lahoz, and Alan Hall

Cell Biology Program, Memorial Sloan-Kettering Cancer Center, New York, NY 10065

KRAS, *BRAF*, and *PI3KCA* are the most frequently mutated oncogenes in human colon cancer. To explore their effects on morphogenesis, we used the colon cancer–derived cell line Caco-2. When seeded in extracellular matrix, individual cells proliferate and generate hollow, polarized cysts. The expression of oncogenic phosphatidylinositol 3-kinase (PI3KCA H1047R) in Caco-2 has no effect, but K-Ras V12 or B-Raf V600E disrupts polarity and tight junctions and promotes hyperproliferation, resulting in large, filled structures. Inhibition of mitogen-activated protein/extracellular signal–regulated kinase (ERK) kinase blocks the disruption of morphology, as well as the increased levels of c-myc protein induced by K-Ras V12 and B-Raf V600E. Apical polarity is already established after the first cell division (two-cell stage) in Caco-2 three-dimensional cultures. This is disrupted by expression of K-Ras V12 or B-Raf V600E but can be rescued by ribonucleic acid interference–mediated depletion of c-myc. We conclude that ERK-mediated up-regulation of c-myc by K-Ras or B-Raf oncogenes disrupts the establishment of apical/basolateral polarity in colon epithelial cells independently of its effect on proliferation.

Introduction

Human colorectal carcinomas have the third highest incidence and are the second most common cause of cancer-related deaths in both men and women (U.S. Cancer Statistics Working Group, 2010). The genetics of colorectal tumors have been extensively studied and defined by a series of stepwise alterations, including disruption of the tumor suppressor functions of APC, p53, and SMAD2/4 (Vogelstein et al., 1988; Fearon and Vogelstein, 1990). The Catalogue of Somatic Mutations in Cancer has revealed that the three most commonly mutated oncogenes in colorectal carcinoma are *KRAS* (35%) and its effectors *BRAF* (12%) and *PI3KCA* (12%; Forbes et al., 2011). Interestingly, colorectal tumors rarely contain both *KRAS* and *BRAF* mutations, although ∼8% have *PI3KCA* mutations coexistent with *KRAS* or *BRAF* mutations (Rajagopalan et al., 2002; Yuan and Cantley, 2008; Janku et al., 2011).

We have developed a 3D model of morphogenesis with the colon cancer–derived cell line, Caco-2 (Jaffe et al., 2008). Caco-2 cells harbor mutations in *APC*, *p53*, and *SMAD4* but not in *KRAS*, *BRAF*, or *PI3KCA*. (De Bosscher et al., 2004; Forbes et al., 2011). These cells have been used extensively to study normal and differentiated intestinal epithelium in 2D culture (Grasset et al., 1985; Sääf et al., 2007). When seeded in extracellular matrix containing laminin and collagen, Caco-2 cells form fully polarized cysts that have tight junctions and membrane polarity. Cyst development involves oriented, symmetric cell divisions, such that each new daughter maintains contact with a central apical surface to produce a polarized spherical monolayer (Jaffe et al., 2008). Interestingly, apical/basolateral polarity and tight junction formation are established at the two-cell stage in 3D, likely during or soon after cytokinesis in the first cell division.

3D epithelial cell culture systems provide an opportunity to explore the effects of oncogene expression on morphogenesis, alongside proliferation and growth (Debnath and Brugge, 2005). To date, most work in this area has been conducted with mammary epithelial cells. Activated ErbB2, active AKT, or ectopic c-myc expression in the human breast cancer cell line MCF10A, for example, promotes hyperproliferation and disrupts cyst

Correspondence to Alan Hall: halla@mskcc.org

Abbreviations used in this paper: aPKC, atypical PKC; ERK, extracellular signal–regulated kinase; MEK, MAP/ERK kinase; PI3K, phosphatidylinositol 3-kinase; RB, retinoblastoma; shRNA, small hairpin RNA.

The Rockefeller University Press $30.00
J. Cell Biol. Vol. 198 No. 2 185–194
www.jcb.org/cgi/doi/10.1083/jcb.201202108

morphogenesis in 3D cultures (Muthuswamy et al., 2001; Debnath et al., 2003; Zhan et al., 2008; Partanen et al., 2009). Further analysis suggested that disruption of cyst morphology and the promotion of proliferation are distinct activities of ErbB2—the former mediated by an interaction of this receptor with the apical polarity complex Par6–atypical PKC (aPKC; Aranda et al., 2006). However, MCF10A cells lack tight junctions, caused by low levels of the apical polarity protein Crumbs, and so are not fully polarized (Fogg et al., 2005; Underwood et al., 2006; Plachot et al., 2009). Primary mouse mammary cells do form fully polarized cysts with tight junctions when grown in a 3D matrix (Jechlinger et al., 2009). In this case, expression of the K-Ras V12 oncogene, together with c-myc, led to large, filled 3D structures, but the relationship between dysregulated proliferation and disruption of morphogenesis was not addressed in this study. Other epithelial cell types, such as lung, colon, and pancreas, have been used in 3D culture conditions, but whether disruption of morphogenesis is a direct effect of oncogene signaling or an indirect consequence of hyperproliferation is unclear (Wang et al., 2009; Makrodouli et al., 2011; Botta et al., 2012).

Here, we report that expression of the K-Ras or B-Raf oncogenes induces hyperproliferation and disrupts morphogenesis in Caco-2 3D cultures. Both oncogenes inhibit the establishment of apical polarity and tight junctions in two-cell structures, and this is mediated through increased levels of c-myc protein. We conclude that the K-Ras and B-Raf oncogenes disrupt apical/basolateral polarity in colon epithelial cells independently of their effects on proliferation.

Results and discussion

Oncogenic K-Ras and B-Raf disrupt Caco-2 3D morphogenesis

Previous work has shown that Caco-2 cells seeded in extracellular matrix generate hollow, fully polarized structures after 10 d (Jaffe et al., 2008; Durgan et al., 2011). These structures show clear apical localization of aPKC, a member of the Par3–Par6–aPKC apical polarity complex, at the inner luminal surface and are categorized as having "normal" morphology (Fig. 1 A and Video 1). Caco-2 cells expressing an oncogenic version of phosphatidylinositol 3-kinase (PI3K; PI3KCA H1047R) form structures identical to control (Fig. 1, A and B, left). In contrast, Caco-2 cells expressing K-Ras V12 or B-Raf V600E produce filled structures that lack a central lumen and are categorized as "solid" (Fig. 1, A and B, left; and Video 2). These structures show diffuse cytoplasmic staining of aPKC with occasional small patches of aPKC membrane localization. An intermediate category of "multiple layer" describes structures that have a lumen but with multiple cell layers between the apical surface and the outer edge of the structure. K-Ras V12 and B-Raf V600E structures are also much larger than controls (Fig. 1, A and B, right). The functional activity of these expressed oncogenes was confirmed by Western blot analysis, and the expression level of B-Raf V600E is similar (1.5×) to endogenous B-Raf (Fig. S1 A). In a recent publication, B-Raf V600E was also reported to produce solid structures when expressed in Caco-2 in 3D cell culture, but K-Ras V12 had no effect (Makrodouli et al., 2011). The reason for this discrepancy is not clear—perhaps the two Caco-2 isolates differ, or perhaps the level of oncogene expression is a factor.

K-Ras V12 promotes hyperproliferation and disrupts apical polarity and tight junction formation

To further characterize the effect of K-Ras V12 expression, cells were reextracted from 3D matrix 10 d after plating, and lysates were analyzed by Western blotting. As expected, increased levels of phospho–extracellular signal–regulated kinase (ERK) and phospho-AKT were apparent (Fig. 2 A). Control cells proliferate for several days when grown in 3D matrix (Fig. 2 B) but then exit the cell cycle (Fig. 2 C). This phenomenon has been attributed to contact inhibition followed by differentiation in 2D cultures (Sääf et al., 2007), but it is not clear why Caco-2 cells stop proliferating in 3D cultures. K-Ras V12–expressing cells, on the other hand, continue to proliferate over a period of ≥10 d, and Ki67 expression suggests that proliferation occurs in cells irrespective of whether they are positioned internally or peripherally (Fig. 2, B and C).

To investigate the effects of K-Ras V12 expression on cell polarity, immunofluorescence was performed on day 10 structures. The apical markers aPKC and ezrin strongly localize to the luminal surface of control structures, but this is disrupted after K-Ras V12 expression, and the proteins become largely cytoplasmic (Fig. 2, D and E). Although apical localization of actin is also disrupted after K-Ras V12 expression (Fig. 2 D), K-Ras V12 appears to have little effect on the deposition of laminin on the outside of peripheral cells (Fig. 2 E). E-cadherin, which localizes to lateral membranes in control cells, remains membrane bound in K-Ras V12 structures (protein levels are unaffected by Western blot analysis; not depicted) but becomes evenly distributed around the periphery of all cells (Fig. 2 F). ZO-1 localizes to the apical tip of the lateral membrane in control cells and is essential for luminal expansion. This is largely absent in K-Ras structures (Fig. 2 F). We conclude that K-Ras and B-Raf (unpublished data) oncogenes promote hyperproliferation and disrupt apical polarity and tight junction formation when expressed in Caco-2 cells.

Mitogen-activated protein/ERK kinase (MEK) inhibition prevents K-Ras V12–mediated disruption of normal morphology

To identify signals downstream of K-Ras V12 responsible for these effects, inhibitors of MEK (component of the ERK MAPK pathway) and PI3K were used, and their effectiveness was shown on Western blots (Fig. S1 B). Increasing concentrations of the MEK inhibitor U0126 from 5 to 20 µM prevented K-Ras V12 from promoting hyperproliferation and from disrupting Caco-2 3D morphology (Fig. 3, A and B). At the highest concentration of U0126, and after 10 d, the size and morphology of K-Ras V12 structures were almost indistinguishable from those of control cells. Interestingly, if the MEK inhibitor is washed out of K-Ras V12–expressing cells after a 4-d incubation, the normal morphology of the 3D structures is maintained over the subsequent 3 d (unpublished data). Thus, reactivation of K-Ras

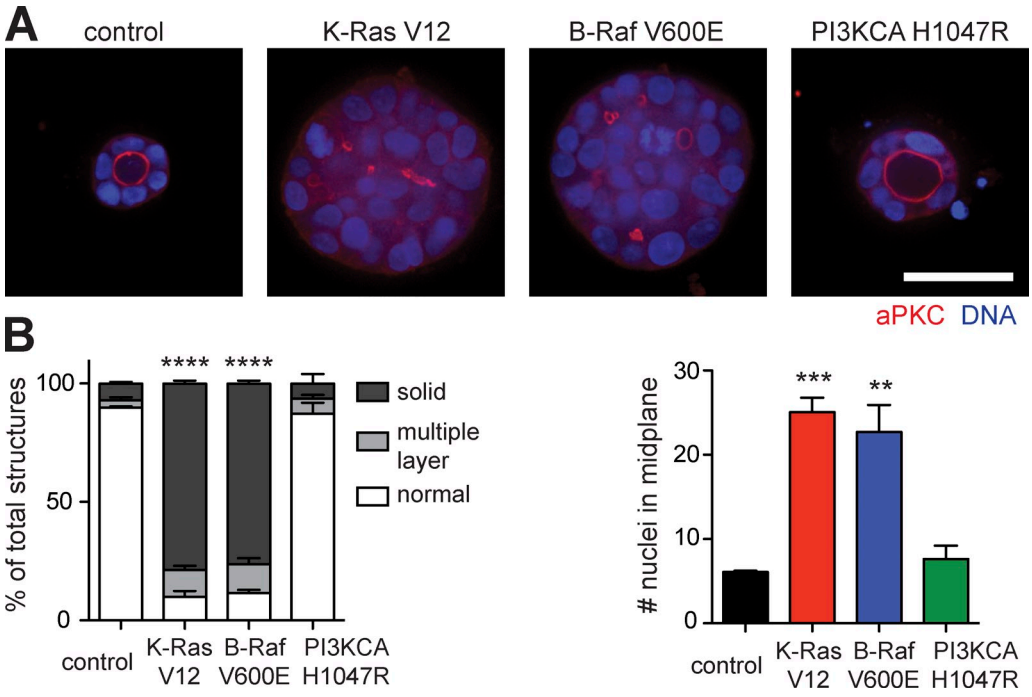

Figure 1. **K-Ras V12 and B-Raf V600E disrupt normal morphogenesis in Caco-2 3D cultures.** (A) 3D cultures expressing control (pQCXIP GFP), K-Ras V12 (pQCXIP GFP K-Ras V12), B-Raf V600E (pQCFLAP B-Raf V600E), or PI3KCA H1047R (pQCFLAP PI3KCA H1047R) were fixed at day 10 and stained for aPKC and DNA. Representative images are shown. Bar, 50 µm. (B) The midplanes of ≥50 structures were imaged for each condition in three independent experiments and categorized as having normal, multiple layer, or solid morphology. The number of nuclei in the midplane of each structure was also quantified. The means ± SEM are shown. **, $P < 0.01$; ***, $P < 0.0005$; ****, $P < 0.0001$.

V12 signaling does not reverse the loss in proliferative capacity exhibited by Caco-2 cells nor does it promote disruption of apical/basal polarity. This supports the idea that the primary effect of K-Ras V12 expression is on polarity establishment rather than polarity maintenance.

In contrast to MEK inhibition, the PI3K inhibitor PIK-90 applied to K-Ras V12 structures at 0.5 µM reduced phospho-AKT levels to below those in control cells (Fig. S1 B) but had no significant effect on the size or morphology of K-Ras V12 structures (Fig. 3 B). At a higher concentration of PIK-90, proliferation was inhibited, but the remaining structures still lacked apical polarity (Fig. 3, A and B). These observations, together with the identical effects of K-Ras V12 and B-Raf V600E, strongly indicate that both hyperproliferation and disruption of epithelial polarity are a consequence of ERK activation.

K-Ras V12 and B-Raf V600E promote hyperproliferation and disrupt morphogenesis through up-regulation of c-myc

ERK activation has a large number of downstream consequences, but numerous studies suggest that a key effector, particularly in the context of cancer, is c-myc (Sears et al., 2000; Lee et al., 2010). To determine whether c-myc protein levels are affected by K-Ras V12 or B-Raf V600E, cells were seeded in 3D culture and, 24 h later, reextracted, lysed, and analyzed on Western blots. K-Ras V12 and B-Raf V600E expression resulted in a 10-fold increase in c-myc protein levels and a corresponding increase in phospho-Ser62 c-myc (Fig. 4 A and Fig. S2 A). Furthermore, the increase in c-myc levels is completely inhibited upon MEK inhibition of K-Ras V12– and B-Raf V600E–expressing cells (Fig. 4 A and Fig. S2 B). Phosphorylation of c-myc by ERK on Ser62 has been shown to promote c-myc stabilization (Sears et al., 2000). This likely accounts for the increased levels of protein observed, although c-myc levels can also be regulated at the transcriptional and translational levels, and we have observed a 2.5-fold increase in c-myc mRNA levels in K-Ras V12 and B-Raf V600E 3D cultures as determined by quantitative PCR (Fig. S2 C).

To determine whether the increased levels of c-myc mediate any of the biological effects of K-Ras V12 or B-Raf V600E expression, two c-myc small hairpin RNAs (shRNAs) were used. Hairpin 2 substantially depleted c-myc levels, whereas Hairpin 1 depletion was partial (Fig. S2 D). Hairpin 2 fully prevented both the disruption of morphology and the hyperproliferation induced by K-Ras V12 and B-Raf V600E expression, whereas Hairpin 1 was partially effective (Fig. 4, B and C).

To determine whether c-myc alone is sufficient to disrupt Caco-2 3D morphogenesis and promote hyperproliferation, c-myc was expressed in cells from a retroviral vector. After selection, the level of c-myc expression in Caco-2 cells was similar to that found in K-Ras V12–expressing cells (Fig. 4 F). c-myc expression disrupted Caco-2 morphology to produce solid structures and had a modest effect on the overall size of the structure (Fig. 4, D and E). Because c-myc expression is known to increase both proliferation and apoptosis, it is likely that other signals prevent c-myc–dependent apoptosis in K-Ras V12 and B-Raf V600E 3D structures (Evan et al., 1992; Zhan et al., 2008). We conclude that both the disruption of cell polarity and the promotion of hyperproliferation by K-Ras and B-Raf oncogenes are mediated by up-regulation of c-myc.

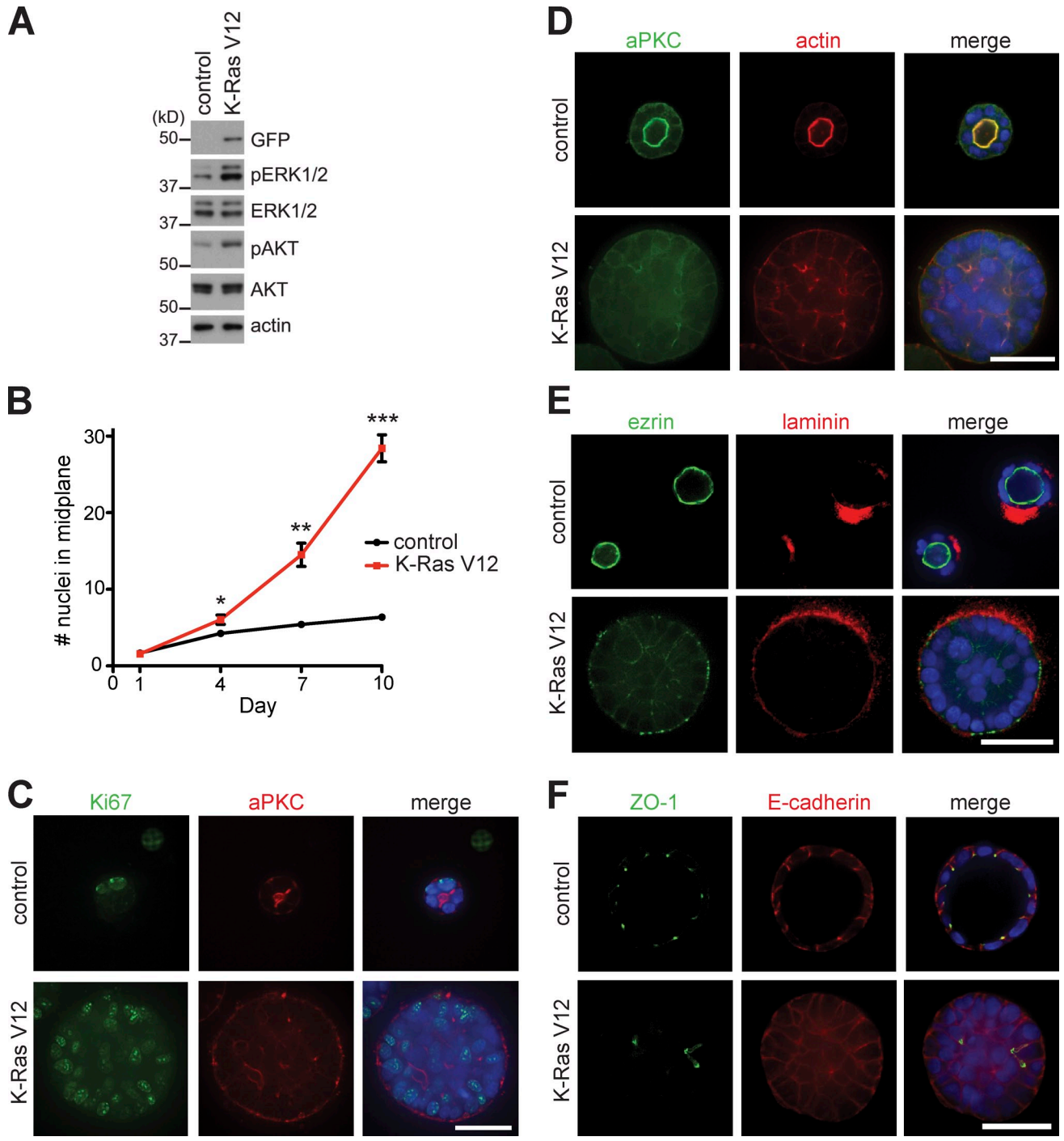

Figure 2. **K-Ras V12 expression disrupts apical polarity and tight junctions and promotes hyperproliferation.** (A) Day 10 3D cultures expressing control (pQCXIP GFP) or K-Ras V12 (pQCXIP GFP K-Ras V12) were lysed and analyzed by Western blotting with the indicated antibodies. (B) Day 1, 4, 7, and 10 3D cultures expressing control (pQCXIP GFP) or K-Ras V12 (pQCXIP GFP K-Ras V12) were fixed and stained with actin and DNA. The number of nuclei in the midplane of ≥50 structures was determined for each condition in three independent experiments. The means ± SEM are shown. *, $P < 0.05$; **, $P < 0.005$; ***, $P < 0.0005$. (C–F) Day 10 3D structures expressing control (pQCXIP GFP) or K-Ras V12 (pQCXIP GFP K-Ras V12) were fixed and stained for Ki67, aPKC, and DNA (blue; C); aPKC, actin, and DNA (blue; D); ezrin, laminin, and DNA (blue; E); and ZO-1, E-cadherin, and DNA (blue; F). Representative images are shown. Bars, 50 µm.

K-Ras V12 and B-Raf V600E inhibit apical/basolateral polarity establishment at the two-cell stage

To investigate whether the loss of apical polarity and tight junction assembly seen in mature K-Ras V12 and B-Raf V600E structures is a direct effect of increased c-myc expression or an indirect consequence of dysregulated proliferation, 3D cultures were examined after the first cell division in 3D, i.e., at the two-cell stage. The majority of two-cell structures formed from control cells show strong localization of aPKC in an apical domain between the two daughter cells (Fig. 5 A). However, in two-cell structures formed from K-Ras V12– or B-Raf

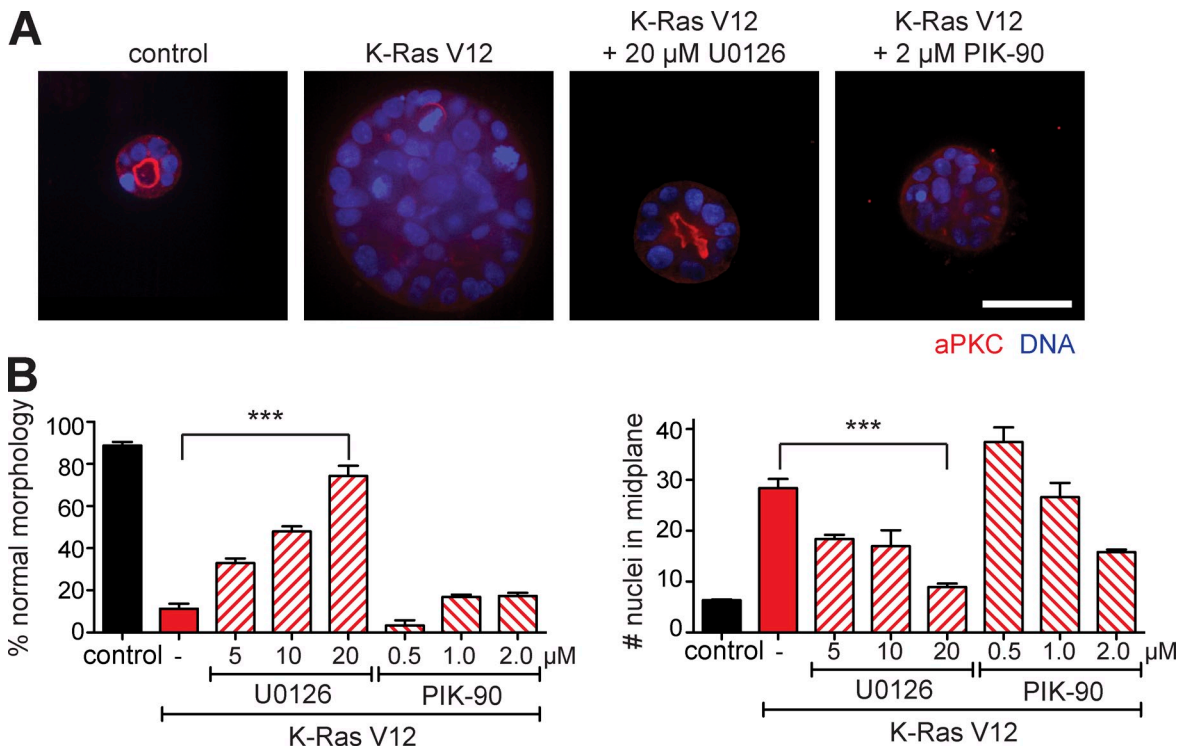

Figure 3. **MEK inhibition prevents K-Ras V12–mediated disruption of normal morphology.** (A) 3D cultures expressing control (pQCXIP GFP) or K-Ras V12 (pQCXIP GFP K-Ras V12) were continuously treated with 5, 10, or 20 μM of the MEK inhibitor U0126 or 0.5, 1.0, or 2.0 μM of the PI3K inhibitor PIK-90. At day 10, these structures were fixed and stained for aPKC and DNA. Representative images are shown. Bar, 50 μm. (B) The midplanes of ≥50 structures were imaged for each condition in three independent experiments. Both the proportion of structures with normal morphology and the number of nuclei in the midplane of each structure were quantified. The means ± SEM are shown. ***, $P < 0.0005$.

V600E–expressing cells, aPKC localization is disrupted, and less than half of the structures are correctly polarized (Fig. 5, A, C, and D). The localization of actin, ZO-1, and E-cadherin is also disrupted (Fig. 5, A and B). MEK inhibition or depletion of c-myc (with shmyc 2) completely restored normal polarity (Fig. 5, C, E, and F). Finally, c-myc overexpression alone significantly inhibited apical polarity establishment at the two-cell stage (Fig. 5, C and G). The inhibition of two-cell polarity establishment by c-myc overexpression was less striking than in K-Ras V12 or B-Raf V600E cells, but this is caused in part, at least, by <50% of the cells expressing increased levels of c-myc, as judged by immunofluorescence (unpublished data).

To further confirm that disruption of polarity establishment is not a result of cell cycle dysregulation, we first analyzed the levels of cell cycle proteins in 3D structures at the two-cell stage. The levels of cyclin A, B, and E and cell cycle inhibitors p16, p21, and p27 were not significantly different in K-Ras V12 or B-Raf V600E cells from control cells, but cyclin D1 levels and retinoblastoma (RB) phosphorylation were significantly increased (Fig. S3 A). However, in c-myc–overexpressing cells, cyclin D1 levels were not significantly different from control cells. In addition, overexpression of cyclin D1 in Caco-2 cells did not disrupt polarity establishment at the two-cell stage (Fig. S3, B, C, and E). The kinase associated with cyclin D1, cdk4, promotes G1 progression and is responsible for RB phosphorylation. Inhibition of cdk4 with the small molecule PD0332991 blocked cell cycle progression, as expected, but at intermediate concentrations, there was no significant increase in normal polarized morphology of K-Ras V12 3D structures (Fig. S3, D and F). Together, these observations are consistent with the conclusion that disruption of polarity establishment is a direct effect of oncogene expression and not an indirect consequence of dysregulated proliferation.

These data show that the K-Ras V12 and B-Raf V600E oncogenes, which are frequently found in human colon cancer, disrupt apical polarity and tight junctions and promote hyperproliferation in Caco-2 cells. All the effects observed are mediated through ERK-dependent up-regulation of c-myc protein. The analysis of two-cell 3D structures reveals that c-myc disrupts the establishment of polarity during the first cell division. The establishment of apical polarity is critical in epithelial cells—it is required to orient the mitotic spindle to promote symmetric cell division within the plane of a tissue, and it is required to establish tight junctions and maintain a distinct luminal surface (Jaffe et al., 2008). In the absence of an apical surface, the orientation of cell divisions becomes randomized, creating a solid or multilayered structure. Although c-myc is up-regulated in a large number of human cancer types, including colon, and is well known to promote hyperproliferation, it was surprising to find that it directly influences polarity establishment in epithelial cells (Bourhis et al., 1990; Kozma et al., 1994; Deming et al., 2000). c-myc is a master regulator known to both activate and repress gene expression, and so it seems likely that changes in one or more of its transcriptional targets are responsible for the effects of c-myc described here on polarity (Brenner et al., 2005).

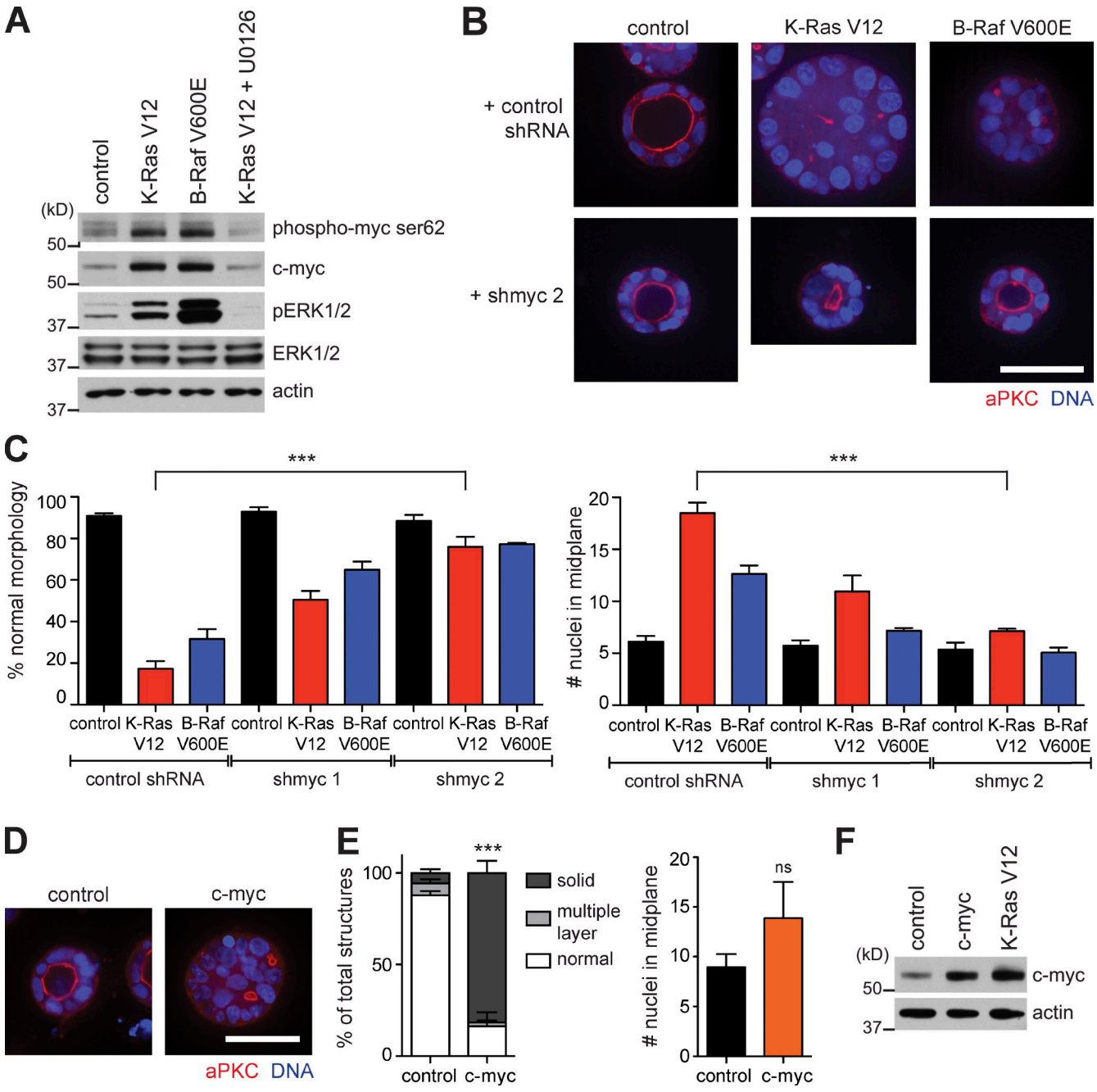

Figure 4. **c-myc mediates the disruption of morphogenesis by K-Ras V12 and B-Raf V600E.** (A) Day 1 3D cultures expressing control (pQCXIP GFP), K-Ras V12 (pQCXIP GFP K-Ras V12), B-Raf V600E (pQCFLAP B-Raf V600E), and K-Ras V12 + 20 µM U0126 were lysed and analyzed by Western blotting with the indicated antibodies. (B) 2 d after infection with either control shRNA or shmyc 2 lentivirus, cells were selected with puromycin for 4 d to make stable cell pools. These cells were superinfected with control (pQCXIP GFP), K-Ras V12 (pQCXIP GFP K-Ras V12), or B-Raf V600E (pQCFLAP B-Raf V600E) retrovirus. 4 d later, cells were seeded into 3D culture. Day 10 3D structures were fixed and stained for aPKC and DNA. Representative images are shown. (C) The midplanes of ≥50 structures were imaged for each condition in three independent experiments. Both the proportion of structures with normal morphology and the number of nuclei in the midplane of each structure were quantified. The means ± SEM are shown. ***, $P < 0.001$. (D) Day 10 3D structures expressing control (uninfected) or c-myc (pBABE blast c-myc) were fixed and stained for aPKC and DNA. Representative images are shown. (E) The midplanes of ≥50 structures were imaged for each condition in three independent experiments and categorized as having normal, multiple layer, or solid morphology. The number of nuclei in the midplane of each structure was also quantified. The means ± SEM are shown. ***, $P < 0.0005$. ns, $P = 0.2729$. (F) Day 1 3D cultures expressing control (pQCXIP GFP), c-myc (pBABE blast myc), and K-Ras V12 (pQCXIP GFP K-Ras V12) were lysed and analyzed by Western blotting with the indicated antibodies. Bars, 50 µm.

Materials and methods

Reagents and antibodies

Primary antibodies used for immunofluorescence are as follows: aPKC (C-20; Santa Cruz Biotechnology, Inc.) at 1:200, Ki67 (M7240; Dako; gift from F. Giancotti, Memorial Sloan-Kettering Cancer Center, New York, NY) at 1:200, E-cadherin (13–1900; Invitrogen) at 1:500, ezrin (E13420; BD) at 1:250, laminin B2 (clone A5; EMD Millipore) at 1:100, and ZO-1 (33–9100; Invitrogen) at 1:500. Secondary antibodies used for immunofluorescence are as follows: Alexa Fluor 488 and 568 (Invitrogen) at 1:200, Cy3 (Jackson

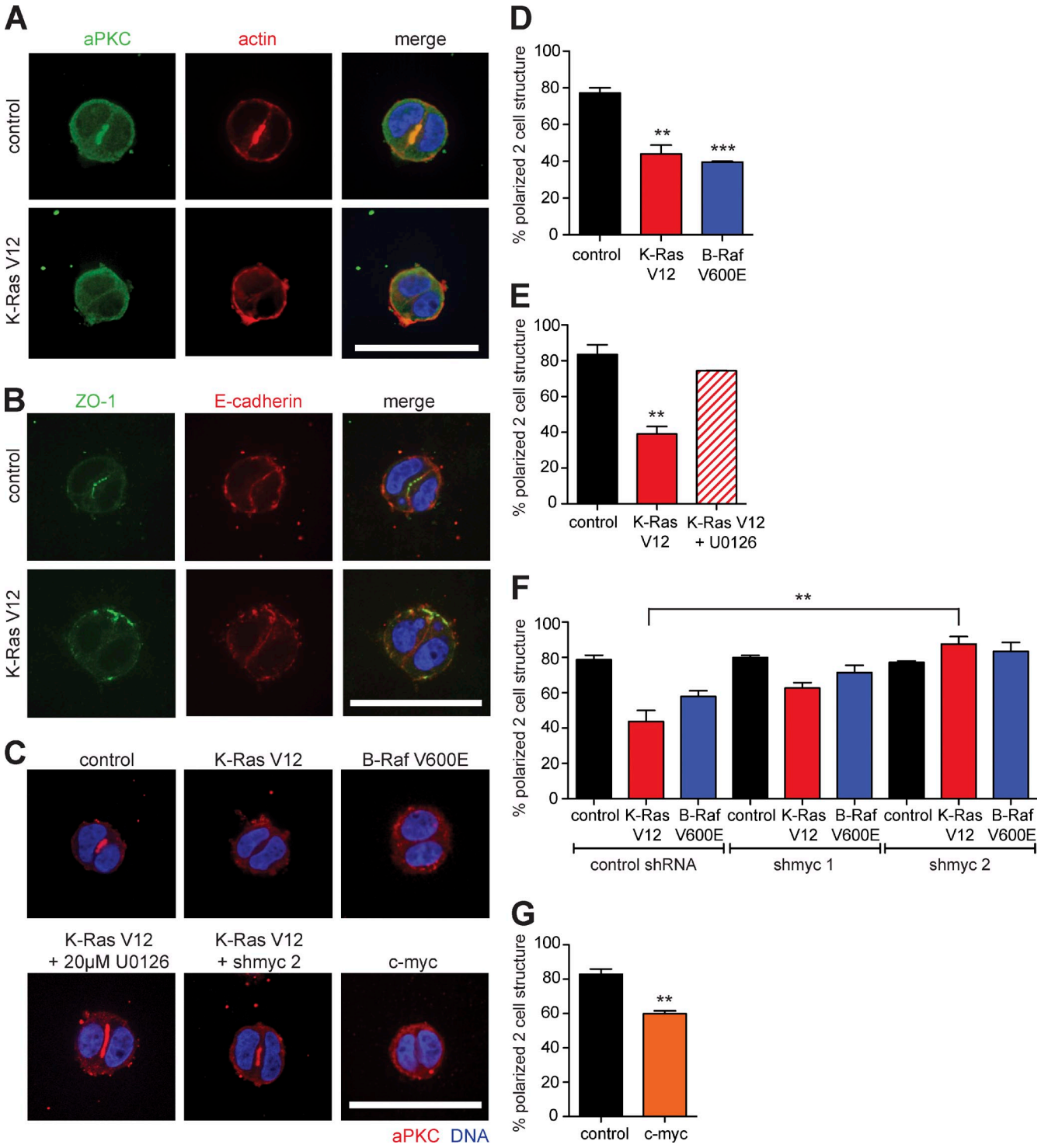

Figure 5. **K-Ras V12 and B-Raf V600E inhibit apical polarity establishment through ERK-mediated regulation of c-myc.** (A and B) Single cells expressing control (pQCXIP GFP) or K-Ras V12 (pQCXIP GFP K-Ras V12) were embedded in matrix. After 2 d, cells were fixed and stained for aPKC, actin, and DNA (blue; A) and ZO-1, E-cadherin, and DNA (blue; B). Representative images are shown. (C) Two-cell structures expressing control (pQCXIP GFP), K-Ras V12 (pQCXIP GFP K-Ras V12), B-Raf V-600E (pQCFLAP B-Raf V600E), or c-myc (pBabe blast c-myc) were fixed and stained for aPKC and DNA. (bottom) K-Ras V12–expressing Caco-2 cells were plated as single cells in 3D and treated with 20 μM U0126. Cells stably expressing shmyc 2 were superinfected with K-Ras V12 (pQCXIP GFP K-Ras V12) retrovirus. 4 d later, cells were seeded into 3D culture. Cells were fixed 2 d later at the two-cell stage and stained for aPKC and DNA. Representative images are shown. (D–G) At least 50 two-cell structures were imaged for each condition in three independent experiments and analyzed for proper apical localization of aPKC. The means ± SEM are shown. **, $P < 0.005$; ***, $P < 0.0005$. Bars, 50 μm.

ImmunoResearch Laboratories, Inc.) at 1:200, and Cy5 (Jackson ImmunoResearch Laboratories, Inc.) at 1:100. Primary antibodies used for Western blotting were AKT (9272; Cell Signaling Technology) at 1:1,000, β-actin (clone AC-74; Sigma-Aldrich) at 1:10,000, B-Raf (C-19; Santa Cruz Biotechnology, Inc.) at 1:1,000, cyclin A (H-432; Santa Cruz Biotechnology, Inc.) at 1:500, cyclin B (H-433; Santa Cruz Biotechnology, Inc.) at 1:500, cyclin D1 (K0062-3; MBL International) at 1:1,000, cyclin E (HE12; Santa Cruz Biotechnology, Inc.), ERK1/2 (M5670; Sigma-Aldrich) at 1:2,000, Flag (clone M2; Sigma-Aldrich) at 1:2,000, GFP (clone 3E1; Cancer Research UK) at 1:1,000, myc (clone 9E10; Cancer Research UK) at 1:1,000, p16 (C-20; Santa Cruz Biotechnology, Inc.; gift from A. Koff, Memorial Sloan-Kettering Cancer Center, New York, NY) at 1:250, p21 (C-19; Santa Cruz Biotechnology, Inc.) at 1:250, p27 (C-19; Santa Cruz Biotechnology, Inc.) used at 1:250, phospho-AKT (4060S; Cell Signaling Technology) at 1:1,000, phospho-ERK (M8159; Sigma-Aldrich) at 1:1,000, phospho-myc (Ser62; 33A12E10; Abcam) at 1:250, phospho-RB (9308; Cell Signaling Technology; gift from F. Giancotti) used at 1:1,000, and RB (C-15; Santa Cruz Biotechnology, Inc.) used at 1:500. Secondary polyclonal antibodies conjugated for HRP for Western blotting were obtained from Dako and used at 1:5,000. Other reagents used were as follows: phalloidin 647 (Invitrogen) at 1:100, DRAQ5 (Cell Signaling Technology) at 1:1,000, Hoechst 33342 (Sigma-Aldrich) at 1 µg/ml, U0126 (Promega), PIK-90 (Selleck Chemicals; gift from M. Overholtzer, Memorial Sloan-Kettering Cancer Center, New York, NY), and PD0332991 (Selleck Chemicals).

Plasmids and cloning

pQCXIP GFP was made by subcloning (Age1–BamH1) GFP from pEGFP-C1 into pQCXIP. K-Ras V12 was subcloned (BamH1) from pBABE K-Ras V12 (Addgene plasmid 9052; W. Hahn, Dana Farber Cancer Institute, Boston, MA) into pQCXIP GFP. B-Raf V600E was amplified by PCR from pBABE B-Raf V600E (Addgene plasmid 17544; Hao et al., 2007) with the following primers that contain attB1 and attB2 Gateway recombination sites: forward, 5′-GGGGACAAGTTTGTACAAAAAAGCAGGCTTCATGGCGGCGCTGAGCGGTGGCG-3′; and reverse, 5′-GGGGACCACTTTGTACAAGAAAGCTGGGTCTCAGTGGACAGGAAACGCACCATATC-3′. PI3KCA H1047R was amplified by PCR from pBABE HA PI3KCA H1047R (Addgene plasmid 12524; Zhao et al., 2005) with the following primers that contain attB1 and attB2 Gateway recombination sites: forward, 5′-GGGGACAAGTTTGTACAAAAAAGCAGGCTTCATGGCGGCGCTGAGCGGTGGCG-3′; and reverse, 5′-GGGGACCACTTTGTACAAGAAAGCTGGGTCTCAGTTCAATGCATGCTGTTTAATTGTGT-3′. B-Raf V600E and PI3KCA H1047R were recombined into pQCFLAP, a derivative of pQCXIN with Gateway att sites, GFP, and Flag tags (obtained from P. Jallepalli, Memorial Sloan-Kettering Cancer Center, New York, NY). pWZL blast c-myc was obtained from Addgene (plasmid 10674; Boehm et al., 2005). pBABE puro cyclin D1 was obtained from J. Brugge (Harvard Medical School, Boston, MA; Debnath et al., 2002).

Cell culture

Caco-2 cells were cultured in DME with sodium pyruvate (Memorial Sloan-Kettering Cancer Center core facility) supplemented with 10% FCS and antibiotics at 37°C in 5% CO_2. Because there have been conflicting studies about the status of *BRAF*, we sequenced the genomic *BRAF* locus to confirm that our Caco-2 cells are *BRAF* wild type (Oliveira et al., 2003; Hao et al., 2007). To culture mature Caco-2 3D structures, 4-well coverglass-bottom slides (Labtek) were coated with 10 µl of a mix of 80% Matrigel (growth factor reduced; BD) and 20% collagen I (Cultrex) and incubated at 37°C for 30 min to solidify. A single-cell suspension (10^4 cells) containing 2% Matrigel was added to each coated well, and cultures were incubated for 10 d before being fixed and stained. To culture two-cell structures, 5×10^3 Caco-2 cells were embedded in a final concentration of 40% Matrigel, 1 mg/ml collagen I, and 0.02 M Hepes in 8-well chamber slides (BD). This mixture was solidified at 37°C and overlaid with 400 µl media and then incubated for 2 d before being fixed and stained.

RNAi

Plasmids encoding shRNA to deplete c-myc and a control shRNA vector (SHC002) were obtained from Sigma-Aldrich. The sequence of shmyc 1 was 5′-CCGGCAGTTGAAACACAAACTTGAACTCGAGTTCAAGTTTGTGTTTCAACTGTTTTTG-3′ (TRCN0000039640). The sequence of shmyc 2 was 5′-CCGGCCTGAGACAGATCAGCAACAACTCGAGTTGTTGCTGATCTGTCTCAGGTTTTTG-3′ (TRCN0000174055).

Virus production, infection, and selection

293FT cells were cultured in high glucose DME (Gibco/Invitrogen) supplemented with 10% FBS, antibiotics, and 2 mM L-glutamine (Invitrogen) at 37°C in 5% CO_2. Cells were grown to 90% confluency in 10-cm plates and transfected with 3 µg VSVG and either 3 µg pCPG gag pol and 3 µg retroviral vector for retrovirus production or 3 µg pDeltaR8.9 and 3 µg shRNA DNA construct for lentivirus production. The transfection reagent used was Lipofectamine LTX with the Plus reagent (Invitrogen) and Opti-MEM (Invitrogen). The medium on the cells was changed to be serum and antibiotic free before the transfection mix was added. After 3 h, the media were removed, and Caco-2 media were added. Virus-containing media were centrifuged at 900 rpm for 3 min and passed through a 0.45-µm filter (Sarstedt). For control, K-Ras V12, B-Raf V600E, and c-myc retrovirus, purified viral supernatants were aliquoted and stored at −80°C. For PI3KCA H1047R retrovirus and shRNA lentivirus, the purified viral supernatant was centrifuged for 2 h at 19,000 rpm at 4°C. The resulting virus pellet was resuspended in PBS, aliquoted, and stored at −80°C.

In preparation for infection, 1.5×10^5 Caco-2 cells were plated per well of 6-well plates. Virus concentrated in PBS was diluted to 1.5 ml in serum- and antibiotic-free medium. All viral mixes were supplemented with 8 µg/ml polybrene (Sigma-Aldrich) before being added to the plates and centrifuged for 30 min at 2,250 rpm. The viral media were discarded and replaced by fresh media. Selection was started 2 d later with 3 µg/ml puromycin (Sigma-Aldrich), 0.7 mg/ml G418 (EMD Millipore), or 5 µg/ml blasticidin (Invitrogen).

Protein analysis

To collect 3D cultures for Western blotting, a single-cell suspension containing 10% Matrigel was plated on ultralow attachment plates (Corning) and collected by resuspension in ice-cold PBS containing 5 mM EDTA and 1 mM sodium orthovanadate (Fournier et al., 2006). This suspension was centrifuged at 900 rpm for 3 min and rinsed with ice-cold PBS containing 1 mM sodium orthovanadate. The resulting pellet was lysed in ice-cold buffer (1% NP-40, 0.1% SDS, 50 mM Tris-HCl, pH 7.5, 150 mM NaCl, 2 mM EDTA, 5 mM Na_3VO_4, and 10 mM NaF) containing protease inhibitors (Roche). Cell lysates were centrifuged at 18,000 *g* for 5 min at 4°C, and the supernatant was immediately processed for SDS-PAGE and Western blotting. For lysis from 2D cell culture, cells were washed with ice-cold PBS containing 1 mM sodium orthovanadate and processed as described for 3D cultures.

Lysates were loaded on 4–12% Bis-Tris gels (Invitrogen) and run with MOPS buffer (Invitrogen). Gels were transferred onto nitrocellulose (Whatman) using transfer buffer (Boston BioProducts) containing 20% methanol (Thermo Fisher Scientific) for 1.25 h at 4°C on ice at 100 V. Membranes were blocked in TBS (Thermo Fisher Scientific) containing 0.1% Tween 20 (Sigma-Aldrich) and 5% milk. Primary antibodies were incubated overnight at 4°C in blocking buffer. Membranes were rinsed 3× for 15 min, incubated with HRP-conjugated secondary antibodies for 1 h, and rinsed 4× for 10 min before a 1-min incubation with ECL (GE Healthcare) and exposure onto film. Bands were quantified using ImageJ (National Institutes of Health).

Immunofluorescence and imaging

Before fixation, embedded 3D cultures were incubated with 50 U/ml collagenase I (Sigma-Aldrich) diluted in PBS for 15 min at RT. Both embedded and mature structures were fixed in 10% formalin (Sigma-Aldrich) for 30 min at RT. After triple washes with PBS, cells were incubated with immunofluorescence buffer (131 mM NaCl, 7 mM dibasic heptahydrate, 3 mM monobasic monohydrate, 8 mM sodium azide, 0.1% BSA, 0.2% Triton X-100, and 0.02% Tween 20) for 15 min at RT. Cells were next incubated in immunofluorescence buffer supplemented with 0.5% Triton X-100 and 1% BSA for 15 min at RT followed by triple washes of PBS. Primary antibody incubation was prepared in PBS with 1% BSA and left at RT for 2 h for embedded structures or overnight at 4°C for mature structures. Cells were then rinsed with PBS 3× for 10 min before secondary fluorescent antibody incubation in PBS with 1% BSA along with phalloidin and a DNA stain of either Hoechst or DRAQ5. Cells were again rinsed with PBS 3× for 10 min. Embedded structures were mounted on coverslips using fluorescent mounting medium (Dako). Mature structures were stored in PBS containing 0.2% azide. This protocol was modified from a previously published study (Jaffe et al., 2008).

Fixed and stained 3D cultures were imaged on a spinning-disk confocal microscope (UltraVIEW ERS; PerkinElmer) with an EM charge-coupled device camera (iXon+ 897; Andor Technology). Mature structures were imaged using a 40× objective (Plan Neofluar, NA 1.3, oil; Carl Zeiss), whereas embedded structures were imaged using a 63× objective (Plan Apochromat, NA 1.4, oil; Carl Zeiss). All imaging was performed with oil immersion at RT. Images were acquired and analyzed with MetaMorph (Molecular Devices). MetaMorph was also used to adjust the brightness and contrast of images as well as to make videos from confocal z stacks.

Quantitative PCR

Cells were cultured as described for 3D lysates. Total cellular RNA was isolated from pellets of day 1 3D structures with a purification kit (RNeasy Mini; QIAGEN). RT-PCR was performed on 200 ng of total RNA using a RT-PCR kit (SuperScript One-Step; Invitrogen) for each sample. Quantitative PCR was performed using TaqMan reagents on the real-time PCR system (7500; Applied Biosystems). The Taqman probe Hs00905030_m1 was used to amplify c-myc, and Hs99999905_m1 was used to amplify glyceraldehyde 3-phosphate dehydrogenase.

Statistics

Statistical significance was evaluated using Prism software (GraphPad Software). The unpaired *t* test was performed with two-tailed p-values and 95% confidence intervals.

Online supplemental material

Fig. S1 shows Western blot analysis of K-Ras V12, B-Raf V600E, and PI3KCA H1047R cell lysates and effects of U0126 or PIK-90 inhibitors. Fig. S2 shows c-myc up-regulation and RNAi depletion in K-Ras V12 and B-Raf V600E cells. Fig. S3 shows that promoting proliferation in control cells or inhibiting proliferation in K-Ras V12 cells does not affect 3D morphology. Videos 1 and 2 are stack videos depicting control or K-Ras V12 day 10 3D structures, respectively, stained with actin and DNA. Online supplemental material is available at http://www.jcb.org/cgi/content/full/jcb.201202108/DC1.

We thank S. Fujisawa and Y. Romin (Memorial Sloan-Kettering Cancer Center Molecular Cytology Core) for microscopy assistance, Dr. M. Overholtzer for PIK-90, Dr. P. Jallepalli for the pQCFLAP vector, Dr. F. Giancotti for Ki67 and phospho-RB antibodies, Dr. A. Koff for p16, p27, and RB antibodies, Dr. D. Ciznadija for retinal pigment epithelial cell lysate, and members of the Hall laboratory for helpful discussions.

This work was supported by National Institutes of Health Medical Scientist Training Program grant GM07739 (to K. Magudia) and National Institutes of Health grant GM081435 (to A. Hall).

Submitted: 20 February 2012
Accepted: 14 June 2012

References

Aranda, V., T. Haire, M.E. Nolan, J.P. Calarco, A.Z. Rosenberg, J.P. Fawcett, T. Pawson, and S.K. Muthuswamy. 2006. Par6-aPKC uncouples ErbB2 induced disruption of polarized epithelial organization from proliferation control. *Nat. Cell Biol.* 8:1235–1245. http://dx.doi.org/10.1038/ncb1485

Boehm, J.S., M.T. Hession, S.E. Bulmer, and W.C. Hahn. 2005. Transformation of human and murine fibroblasts without viral oncoproteins. *Mol. Cell. Biol.* 25:6464–6474. http://dx.doi.org/10.1128/MCB.25.15.6464-6474.2005

Botta, G.P., M.J. Reginato, M. Reichert, A.K. Rustgi, and P.I. Lelkes. 2012. Constitutive K-RasG12D activation of ERK2 specifically regulates 3D invasion of human pancreatic cancer cells via MMP-1. *Mol. Cancer Res.* 10:183–196. http://dx.doi.org/10.1158/1541-7786.MCR-11-0399

Bourhis, J., M.G. Le, M. Barrois, A. Gerbaulet, D. Jeannel, P. Duvillard, V. Le Doussal, D. Chassagne, and G. Riou. 1990. Prognostic value of c-myc proto-oncogene overexpression in early invasive carcinoma of the cervix. *J. Clin. Oncol.* 8:1789–1796.

Brenner, C., R. Deplus, C. Didelot, A. Loriot, E. Viré, C. De Smet, A. Gutierrez, D. Danovi, D. Bernard, T. Boon, et al. 2005. Myc represses transcription through recruitment of DNA methyltransferase corepressor. *EMBO J.* 24:336–346. http://dx.doi.org/10.1038/sj.emboj.7600509

Debnath, J., and J.S. Brugge. 2005. Modelling glandular epithelial cancers in three-dimensional cultures. *Nat. Rev. Cancer*. 5:675–688. http://dx.doi.org/10.1038/nrc1695

Debnath, J., K.R. Mills, N.L. Collins, M.J. Reginato, S.K. Muthuswamy, and J.S. Brugge. 2002. The role of apoptosis in creating and maintaining luminal space within normal and oncogene-expressing mammary acini. *Cell*. 111:29–40. http://dx.doi.org/10.1016/S0092-8674(02)01001-2

Debnath, J., S.J. Walker, and J.S. Brugge. 2003. Akt activation disrupts mammary acinar architecture and enhances proliferation in an mTOR-dependent manner. *J. Cell Biol.* 163:315–326. http://dx.doi.org/10.1083/jcb.200304159

De Bosscher, K., C.S. Hill, and F.J. Nicolás. 2004. Molecular and functional consequences of Smad4 C-terminal missense mutations in colorectal tumour cells. *Biochem. J.* 379:209–216. http://dx.doi.org/10.1042/BJ20031886

Deming, S.L., S.J. Nass, R.B. Dickson, and B.J. Trock. 2000. C-myc amplification in breast cancer: a meta-analysis of its occurrence and prognostic relevance. *Br. J. Cancer*. 83:1688–1695. http://dx.doi.org/10.1054/bjoc.2000.1522

Durgan, J., N. Kaji, D. Jin, and A. Hall. 2011. Par6B and atypical PKC regulate mitotic spindle orientation during epithelial morphogenesis. *J. Biol. Chem.* 286:12461–12474. http://dx.doi.org/10.1074/jbc.M110.174235

Evan, G.I., A.H. Wyllie, C.S. Gilbert, T.D. Littlewood, H. Land, M. Brooks, C.M. Waters, L.Z. Penn, and D.C. Hancock. 1992. Induction of apoptosis in fibroblasts by c-myc protein. *Cell*. 69:119–128. http://dx.doi.org/10.1016/0092-8674(92)90123-T

Fearon, E.R., and B. Vogelstein. 1990. A genetic model for colorectal tumorigenesis. *Cell*. 61:759–767. http://dx.doi.org/10.1016/0092-8674(90)90186-I

Fogg, V.C., C.-J. Liu, and B. Margolis. 2005. Multiple regions of Crumbs3 are required for tight junction formation in MCF10A cells. *J. Cell Sci.* 118:2859–2869. http://dx.doi.org/10.1242/jcs.02412

Forbes, S.A., N. Bindal, S. Bamford, C. Cole, C.Y. Kok, D. Beare, M. Jia, R. Shepherd, K. Leung, A. Menzies, et al. 2011. COSMIC: mining complete cancer genomes in the Catalogue of Somatic Mutations in Cancer. *Nucleic Acids Res.* 39(Suppl. 1):D945–D950. http://dx.doi.org/10.1093/nar/gkq929

Fournier, M.V., K.J. Martin, P.A. Kenny, K. Xhaja, I. Bosch, P. Yaswen, and M.J. Bissell. 2006. Gene expression signature in organized and growth-arrested mammary acini predicts good outcome in breast cancer. *Cancer Res.* 66:7095–7102. http://dx.doi.org/10.1158/0008-5472.CAN-06-0515

Grasset, E., J. Bernabeu, and M. Pinto. 1985. Epithelial properties of human colonic carcinoma cell line Caco-2: effect of secretagogues. *Am. J. Physiol.* 248:C410–C418.

Hao, H., V.M. Muniz-Medina, H. Mehta, N.E. Thomas, V. Khazak, C.J. Der, and J.M. Shields. 2007. Context-dependent roles of mutant B-Raf signaling in melanoma and colorectal carcinoma cell growth. *Mol. Cancer Ther.* 6:2220–2229. http://dx.doi.org/10.1158/1535-7163.MCT-06-0728

Jaffe, A.B., N. Kaji, J. Durgan, and A. Hall. 2008. Cdc42 controls spindle orientation to position the apical surface during epithelial morphogenesis. *J. Cell Biol.* 183:625–633. http://dx.doi.org/10.1083/jcb.200807121

Janku, F., J.J. Lee, A.M. Tsimberidou, D.S. Hong, A. Naing, G.S. Falchook, S. Fu, R. Luthra, I. Garrido-Laguna, and R. Kurzrock. 2011. PIK3CA mutations frequently coexist with RAS and BRAF mutations in patients with advanced cancers. *PLoS ONE*. 6:e22769. http://dx.doi.org/10.1371/journal.pone.0022769

Jechlinger, M., K. Podsypanina, and H. Varmus. 2009. Regulation of transgenes in three-dimensional cultures of primary mouse mammary cells demonstrates oncogene dependence and identifies cells that survive deinduction. *Genes Dev.* 23:1677–1688. http://dx.doi.org/10.1101/gad.1801809

Kozma, L., I. Kiss, S. Szakáll, and I. Ember. 1994. Investigation of c-myc oncogene amplification in colorectal cancer. *Cancer Lett.* 81:165–169. http://dx.doi.org/10.1016/0304-3835(94)90198-8

Lee, S.H., L.-L. Hu, J. Gonzalez-Navajas, G.S. Seo, C. Shen, J. Brick, S. Herdman, N. Varki, M. Corr, J. Lee, and E. Raz. 2010. ERK activation drives intestinal tumorigenesis in Apc(min/+) mice. *Nat. Med.* 16:665–670. http://dx.doi.org/10.1038/nm.2143

Makrodouli, E., E. Oikonomou, M. Koc, L. Andera, T. Sasazuki, S. Shirasawa, and A. Pintzas. 2011. BRAF and RAS oncogenes regulate Rho GTPase pathways to mediate migration and invasion properties in human colon cancer cells: a comparative study. *Mol. Cancer*. 10:118. http://dx.doi.org/10.1186/1476-4598-10-118

Muthuswamy, S.K., D. Li, S. Lelievre, M.J. Bissell, and J.S. Brugge. 2001. ErbB2, but not ErbB1, reinitiates proliferation and induces luminal repopulation in epithelial acini. *Nat. Cell Biol.* 3:785–792. http://dx.doi.org/10.1038/ncb0901-785

Oliveira, C., M. Pinto, A. Duval, C. Brennetot, E. Domingo, E. Espín, M. Armengol, H. Yamamoto, R. Hamelin, R. Seruca, and S. Schwartz Jr. 2003. BRAF mutations characterize colon but not gastric cancer with mismatch repair deficiency. *Oncogene*. 22:9192–9196. http://dx.doi.org/10.1038/sj.onc.1207061

Partanen, J.I., A.I. Nieminen, and J. Klefstrom. 2009. 3D view to tumor suppression: Lkb1, polarity and the arrest of oncogenic c-Myc. *Cell Cycle*. 8:716–724. http://dx.doi.org/10.4161/cc.8.5.7786

Plachot, C., L.S. Chaboub, H.A. Adissu, L. Wang, A. Urazaev, J. Sturgis, E.K. Asem, and S.A. Lelièvre. 2009. Factors necessary to produce basoapical polarity in human glandular epithelium formed in conventional and high-throughput three-dimensional culture: example of the breast epithelium. *BMC Biol.* 7:77. http://dx.doi.org/10.1186/1741-7007-7-77

Rajagopalan, H., A. Bardelli, C. Lengauer, K.W. Kinzler, B. Vogelstein, and V.E. Velculescu. 2002. Tumorigenesis: RAF/RAS oncogenes and mismatch-repair status. *Nature*. 418:934. http://dx.doi.org/10.1038/418934a

Sääf, A.M., J.M. Halbleib, X. Chen, S.T. Yuen, S.Y. Leung, W.J. Nelson, and P.O. Brown. 2007. Parallels between global transcriptional programs of polarizing Caco-2 intestinal epithelial cells in vitro and gene expression programs in normal colon and colon cancer. *Mol. Biol. Cell*. 18:4245–4260. http://dx.doi.org/10.1091/mbc.E07-04-0309

Sears, R., F. Nuckolls, E. Haura, Y. Taya, K. Tamai, and J.R. Nevins. 2000. Multiple Ras-dependent phosphorylation pathways regulate Myc protein stability. *Genes Dev.* 14:2501–2514. http://dx.doi.org/10.1101/gad.836800

Underwood, J.M., K.M. Imbalzano, V.M. Weaver, A.H. Fischer, A.N. Imbalzano, and J.A. Nickerson. 2006. The ultrastructure of MCF-10A acini. *J. Cell. Physiol.* 208:141–148. http://dx.doi.org/10.1002/jcp.20639

Vogelstein, B., E.R. Fearon, S.R. Hamilton, S.E. Kern, A.C. Preisinger, M. Leppert, Y. Nakamura, R. White, A.M. Smits, and J.L. Bos. 1988. Genetic alterations during colorectal-tumor development. *N. Engl. J. Med.* 319: 525–532. http://dx.doi.org/10.1056/NEJM198809013190901

Wang, X.-Q., H. Li, V. Van Putten, R.A. Winn, L.E. Heasley, and R.A. Nemenoff. 2009. Oncogenic K-Ras regulates proliferation and cell junctions in lung epithelial cells through induction of cyclooxygenase-2 and activation of metalloproteinase-9. *Mol. Biol. Cell*. 20:791–800. http://dx.doi.org/10.1091/mbc.E08-07-0732

Yuan, T.L., and L.C. Cantley. 2008. PI3K pathway alterations in cancer: variations on a theme. *Oncogene*. 27:5497–5510. http://dx.doi.org/10.1038/onc.2008.245

Zhan, L., A. Rosenberg, K.C. Bergami, M. Yu, Z. Xuan, A.B. Jaffe, C. Allred, and S.K. Muthuswamy. 2008. Deregulation of scribble promotes mammary tumorigenesis and reveals a role for cell polarity in carcinoma. *Cell*. 135:865–878. http://dx.doi.org/10.1016/j.cell.2008.09.045

Zhao, J.J., Z. Liu, L. Wang, E. Shin, M.F. Loda, and T.M. Roberts. 2005. The oncogenic properties of mutant p110alpha and p110beta phosphatidylinositol 3-kinases in human mammary epithelial cells. *Proc. Natl. Acad. Sci. USA*. 102:18443–18448. http://dx.doi.org/10.1073/pnas.0508988102